Regional economic effects of rail infrastructure expansion: Evidence from night-time lights and the Tren Maya in Southern Mexico

Benjamin Aleman-Castilla

Abstract

This paper studies the local economic effects of the Tren Maya railway project using night-time luminosity data and geospatial information on Mexico's rail network. A 2016–2024 panel dataset at the Basic Geostatistical Area level was constructed to exploit variation in proximity to railway infrastructure and to distinguish between general accessibility effects and project-specific impacts associated with the corridor. The empirical strategy combines two-way fixed-effects regressions with event-study estimators that allow for heterogeneous treatment effects over time. Railway accessibility is measured using geodesic distances to rail infrastructure, a composite accessibility index derived from principal component analysis, and spatial buffers around the alignment. Night-time light intensity per square kilometer is used as a proxy for local economic activity. Improved rail accessibility is associated with higher luminosity. Event-study estimates indicate that the effects of the Tren Maya are localized and sensitive to treatment definition. Specifications using narrow spatial buffers satisfy parallel-trends assumptions and yield economically meaningful post-treatment gains. The effects vary across states, with positive impacts in Chiapas, Campeche, and Quintana Roo, no robust effects in Yucatán, and negative effects in Tabasco. These findings suggest that large rail investments can generate localized economic gains, but they are spatially concentrated and context dependent.

JEL Classification: O18, R12, R42

Keywords: Railway infrastructure; Regional economic development; Night-time lights.

Transport has long been regarded as a crucial input for the economic development of nations (The World Bank, 2007). An adequate supply of transportation infrastructure services is a key driver of growth and equity, shaping productivity and access to opportunities (Calderon and Serven, 2010). In Mexico, its role is particularly critical given the country's high degree of trade integration with North America (Moreno-Brid and Ros, 2009; Moreno-Brid *et al.*, 2009; Villarreal and Fergusson, 2017) and the importance of mobility for sustaining both industrial competitiveness and household access to goods and services (Han and Li, 2022; Scholl *et al.*, 2022).

It has been argued that a functional transport sector enables firms to expand markets and reduce costs through economies of scale, fosters inter-firm competition that limits monopolistic pricing, broadens the variety of goods available to consumers, facilitates improved matching between labor skills and job opportunities, and supports the formation of productive agglomerations that enhance innovation and economic growth (Krugman, 1980; Monte *et al.*, 2018; Duranton and Puga, 2023). Likewise, households benefit from lower transport costs and expanded connectivity, which improve quality of life and access to leisure opportunities (Brajša-Žganec *et al.*, 2011; Alhassan and Anciaes, 2025).

Empirically, however, the economic effects of transport infrastructure investments remain ambiguous (Fogel, 1964; Çelik *et al.*, 2025; Ouni *et al.*, 2025). For instance, improvements in connectivity may induce spatial reallocation of capital and labor, potentially concentrating activity in a limited set of industries or locations while leaving others largely unaffected or even worse off (Pi and Wang, 2025). As a result, the net local effects of large transportation projects remain an open question. A growing literature examining the impacts of transport infrastructure finds mixed results (Varghese and

Pradhan, 2025). Studies exploiting quasi-experimental variation in roads, railways, and urban transit systems document positive effects in some contexts but limited or highly localized impacts in others (Donaldson, 2018; Banerjee *et al.*, 2020). Additionally, a recurring challenge in the literature is the endogenous placement of infrastructure, which is often correlated with pre-existing economic trends. Moreover, conventional measures of economic activity at fine spatial scales are typically unavailable or measured with substantial delay. Recent work has addressed these limitations by combining geospatial data with satellite-observed night-time luminosity, which provide a high-frequency and spatially detailed proxy for local economic activity (Gonzalez-Navarro and Turner, 2018; Mitnik *et al.*, 2018).

This paper contributes to this literature by studying the economic effects of the Tren Maya, one of the largest railway infrastructure projects undertaken in Latin America in recent decades. The Tren Maya corridor spans more than 1,500 kilometers across southeastern Mexico and was designed by the federal government to improve connectivity in a region characterized by relatively low income levels and limited transport infrastructure. Since its announcement in 2018, the Tren Maya has generated intense public debate regarding its social, economic and environmental benefits and costs. Yet, despite its scale and policy relevance, there is still limited evidence on its local economic impacts.

The spatial footprint of the Tren Maya is highly heterogeneous. While some segments cross densely populated urban or touristic areas, others pass through sparsely populated rural regions with limited pre-existing transport infrastructure. This heterogeneity in baseline conditions, combined with the clearly defined geographic alignment of the rail corridor and the staggered timing of construction and operation, provides a suitable setting

for evaluating localized economic effects using spatially disaggregated data. In particular, the project's design allows for comparisons between treated and untreated areas at different distances from the rail alignment.

To this end, this study assembles a novel panel dataset combining annual Visible Infrared Imaging Radiometer Suite (VIIRS) night-time light observations at the Basic Geostatistical Area (AGEB, from the Spanish *Área Geoestadística Básica*) level, with high-resolution geospatial data on Mexico's railway network for the period 2016–2024. AGEBs are the fundamental spatial units of Mexico's geostatistical framework and are broadly comparable to census block groups in the United States. Using these data, time-varying measures of proximity and accessibility to railway infrastructure are constructed to examine how changes in access relate to local economic activity. The empirical strategy relies on a combination of two-way fixed-effects (TWFE) regressions and event-study estimators following Callaway and Sant'Anna (2021). A key feature of the analysis is the use of alternative localized treatment definitions, based both on municipalities crossed by the rail alignment and on distance-based buffers around it.

The results point to three main findings. First, improvements in rail accessibility are significantly associated with increases in night-time luminosity at the national level. Second, event-study estimates indicate that the dynamic effects of the Tren Maya depend critically on treatment definition and regional context. In specifications using localized spatial buffers and appropriate control groups, no evidence of differential pre-trends is found, while a temporary decline in luminosity between 2020 and 2021 –consistent with pandemic-related disruptions– is followed by positive responses as construction advanced and operations began in 2024. Disaggregated analyses reveal substantial heterogeneity

across affected states, with positive post-treatment effects in Chiapas, Campeche, and Quintana Roo, no robust gains in Yucatán, and persistent negative effects in Tabasco. Third, at the regional level, the magnitude of the estimated impacts decays with distance to the rail alignment and appears to stabilize toward the onset of operations, suggesting that a significant share of the observed gains might be related to construction-phase activity.

By providing disaggregated evidence on the local economic effects of a major railway project in a developing-country context, this paper contributes to the broader literature on infrastructure and development. Methodologically, it confirms the value of combining remotely sensed data with geospatial information to study infrastructure impacts at a high spatial resolution. From a policy perspective, the findings suggest that while the economic benefits of large rail investments are real, they tend to be geographically concentrated, pointing to the need of complementary interventions to extend their effects more broadly.

The paper is organized as follows: Section II provides an overview of the Tren Maya project. Section III describes the data sources and the construction of the main variables used in the analysis. Section IV outlines the empirical strategy and presents the baseline results. Section V discusses the interpretation of night-time luminosity as a proxy for local economic activity. Section VI examines spatial heterogeneity and state-level effects. Section VII concludes.

I. THE TREN MAYA PROJECT

The Tren Maya is the most relevant rail infrastructure project undertaken in Mexico in recent decades, both for its territorial scale and for its potential economic, social and

environmental impact. It also constitutes a central component of the federal government's infrastructure strategy during the 2018–2024 administration.

Figure 1 here

Conceived as a mixed-use rail corridor, the Tren Maya contemplates a route of approximately 1,554 kilometers across 41 municipalities in the southeastern states of Mexico (see Figure 1): 2 municipalities in Chiapas, 3 in Tabasco, 9 in Campeche, 19 in Yucatán, and 8 in Quintana Roo. Its alignment links major urban centers, tourism hubs, and intermediate localities, including Palenque, Mérida, Cancún, and Tulum. The project was developed and implemented by the federal government through a combination of public investment and enterprises. The National Fund for Tourism Development (FONATUR) served initially as the lead agency, within a government strategy aimed at reducing the historical lags in connectivity, productive integration and regional development that characterize this area of the country (FONATUR, 2020). It was later substituted by the state-owned enterprise Tren Maya, S.A. de C.V., which is sectorized under the Ministry of National Defense (SEDENA).

In contrast to Mexico's existing freight-oriented rail system, the Tren Maya was designed primarily for passenger transport, with complementary freight services in selected segments. It was included in the National Development Plan 2019-2024 and in the sectoral programs of tourism, infrastructure and territorial planning. In this sense, the project was presented as an instrument to strengthen territorial cohesion, improve regional mobility and articulate economic development poles linked to tourism, logistics and services (DOF, 2019). A salient feature of the Tren Maya is that a substantial share of its alignment was

deliberately routed along pre-existing rights of way, most notably the former Chiapas-Mayab railway, approximately 750 kilometers in length, which was concessioned in 1999 to Genesee & Wyoming. Following severe infrastructure damage caused by Hurricane Stan in 2005, operations along this corridor progressively deteriorated and were ultimately abandoned in 2007, leaving an extensive right of way that was subsequently incorporated into the new project. In other sections (such as the 300-km connection between Mérida, Yucatán, and Cancún, Quintana Roo) the alignment follows existing highway corridors or, in some cases, rights of way associated with high-voltage electricity transmission lines (such as in the 250-km section between Chetumal, Quintana Roo, and Escárcega, Campeche). This design strategy aimed to reduce construction costs, mitigate environmental impacts, and minimize land acquisition conflicts, while facilitating project execution. Importantly, it also implies that much of the spatial configuration of the corridor reflects historical infrastructure layouts and engineering constraints rather than contemporaneous patterns of economic activity.

In addition to the rehabilitation of existing tracks and the construction of new ones, the Tren Maya project also included the construction or upgrading of stations, maintenance yards, access roads, and associated urban and logistical infrastructure along the corridor. Even though the project was announced in 2018, construction activities began in 2020, following the completion of preliminary feasibility studies and route definition. The project was divided into seven segments, allowing for staggered construction timelines and phased operation: Palenque, Chiapas – Escárcega, Campeche; Escárcega – Calkiní, Campeche; Calkiní – Izamal, Yucatán; Izamal – Cancún, Quintana Roo; Cancún – Tulum, Quintana Roo; Tulum – Chetumal, Quintana Roo; and Chetumal – Bacalar, Quintana Roo –

Escárcega. Initial sections entered service between 2023 and 2024, while complementary infrastructure and full operational capacity continued to be developed during this period.

Beyond its transport function, the Tren Maya was framed as a regional development intervention, a catalyst for growth and job creation, both in the construction and operation phases. Various technical analyses indicate that the reactivation of rail transport in southeastern Mexico could have beneficial effects for sectors such as tourism, commerce, and services, while also foster the attraction of investment in complementary infrastructure (González *et al.*, 2024). Official project documents emphasize objectives related to reducing transport costs, improving accessibility, promoting tourism diversification, fostering regional supply chains, and stimulating local economic activity in areas adjacent to the rail alignment. However, several specialists have also warned that the economic benefits derived from megaprojects of this nature tend to be unevenly distributed, posing great challenges in terms of social inclusion, territorial equity and protection of the livelihoods of local communities (Cruz *et al.*, 2023; Acevedo *et al.*, 2025).

II. DATA SOURCES AND VARIABLE CONTRUCTION

This study combines satellite-based night-time lights with high-resolution geospatial datasets on railway, road, and economic establishment locations to construct a novel AGEB-level panel for the period 2016–2024. AGEBs are the smallest official statistical unit in Mexico, typically nested within a single municipality (INEGI, 2026a). This section describes each data source and the procedures used to harmonize them into an annual panel.

a. Night-time lights

Night-time luminosity is obtained from the VIIRS Day/Night Band median masked annual composites, produced by the Earth Observation Group at NOAA/NASA's National Polar-Orbiting Partnership–Suomi satellite (Elvidge *et al.*, 2021). These products provide global observations of night-time radiance at high spatial resolution. For each year in the sample, the global VIIRS raster was clipped to the Mexican bounding box (longitude between −120° and −85°, latitude between 14°N and 33°N). Each raster cell was converted into a longitude-latitude-radiance triplet (*lon, lat, rad*), where radiance is measured in nanowatts per square centimeter per steradian (nW/cm^2/sr). The resulting point cloud was projected onto the AGEB polygons from INEGI's 2024 geostatistical framework. Using the same geostatistical framework for all years ensures geographic comparability over time.

For each AGEB i and year t, radiance values $radiance_{it}$ from all VIIRS pixels falling within the polygon were aggregated. Total radiance was computed as the sum of pixel-level radiance $\sum radiance_{it}$, and this quantity was normalized by the area of the AGEB, $area_{it}$, in square kilometers (km^2) to obtain a measure of light density per unit of surface. Given that around 5% of the AGEBs appear with a zero level of radiance in each year of the sample, the inverse hyperbolic sine transformation (IHS) is applied to radiance per square kilometer (Pence, 2006; Mitnik *et al.*, 2018). The IHS transformation is well defined at zero and approximates the logarithmic function for sufficiently large values of light density, facilitating the interpretation of the estimated coefficients. Thus, the main outcome variable is defined as:

$$luminosity_{it} = \ln\left(\frac{\sum radiance_{it}}{area_{it}} + \sqrt{\left(\frac{\sum radiance_{it}}{area_{it}}\right)^2 + 1}\right) \qquad (1)$$

This variable captures changes in the night-time light density per square kilometer, and it is a commonly used proxy to study economic activity and spatial concentration of development in contexts where subnational or more disaggregated statistics are limited (Henderson *et al.*, 2012). Figure 2 illustrates the spatial distribution of changes in luminosity between 2016 and 2024 across Mexico's AGEBs. The map classifies these changes into quartile-based categories, White areas correspond to AGEBs with no observed increase in luminosity or with missing data, while progressively darker shades of blue indicate larger increases in night-time light density. The figure reveals substantial geographic heterogeneity in luminosity growth. Moderate to high increases (third and fourth quartiles) are mostly concentrated in central and northern Mexico. This pattern is consistent with regions that have experienced recent expansion in manufacturing activity, logistics infrastructure, and tourism-related development over the period. Notably, the luminosity growth in southeastern Mexico follows the alignment of the Tren Maya corridor, particularly along the coast of Quintana Roo and in southern Campeche.

Figure 2 here
---

b. Railway infrastructure

Geospatial data on the rail system were sourced from Mexico's Regulatory Agency for Rail Transport (ARTF, 2026). These official datasets consist of five geostatistical vector layers: track geometry (*track*); network junctions or nodes (*node*); yards, terminals and stations (*struct*); functional origin-destination points (*od*), and kilometric markers (*mark*). The layers are available separately for the period 2020–2024 and capture changes in the national rail network over time. Importantly, some of the most recent rail infrastructure

developments –most notably the construction of the Tren Maya corridor– are currently reflected only in the 2024 *track* and *od* layers. Accordingly, these two constitute the primary sources for identifying new rail alignments and operational nodes associated with recent network expansions.

All layers were standardized to the WGS84 coordinate reference system, and their geometries were subsequently decomposed into vertex-level point clouds. For each AGEB i and year t, the minimum geodesic distance between the AGEB centroid and the point clouds corresponding to each rail layer was computed using great-circle nearest-neighbor matching (Picard, 2019), yielding the distance measures $dist_track_{it}$, $dist_node_{it}$, $dist_struct_{it}$, $dist_od_{it}$, and $dist_mark_{it}$. These measures capture the evolving spatial accessibility patters of the rail network, including the Tren Maya corridor, which was first announced by the Mexican federal government in 2018, began its construction phase in 2020, and entered into operation on 15 December 2023.

Table 1 here

Because these variables are strongly correlated (see Table 1), they are additionally summarized into a single accessibility index using Principal Component Analysis (PCA) (Jolliffe, 2002). This procedure extracts orthogonal components PC_i that capture the common variation across the five distance variables. Formally, the accessibility index $rail_{it}$ is constructed as a linear combination of the IHS-transformed geodesic distance measures to the different elements of the railway network:

$$rail_{it} = \sum_{j=1}^{5} \omega_k \tilde{d}_{k,it} \quad (2)$$

where $\tilde{d}_{k,it}$ denotes the IHS transformation of each distance-to-railway variable, and ω_k are their corresponding loadings (that is, the elements of the eigenvector associated with a principal component that indicate the relative importance and direction of each original variable in forming the latent index). As shown in Panel A of Table 2, the first principal component PC_1 explains 81.8% of the total variance across the five distance measures. Panel B reports the individual loadings of the five IHS-transformed distance measures on PC_1. All of them load positively and with similar magnitudes on this component, confirming that the five distances reflect a single underlying dimension. By construction, lower values of $rail_{it}$ correspond to higher rail accessibility, that is, closer proximity to railway infrastructure.

Table 2 here

Figure 3 maps the spatial distribution of changes in proximity to railway infrastructure between 2020 and 2024, as captured by the rail accessibility index $rail_{it}$. Progressively darker shades of blue identify AGEBs experiencing greater reductions in distance to the network. The most pronounced improvements are clearly concentrated along the alignment of the Tren Maya across Campeche, Yucatan, Quintana Roo, Tabasco, and northeastern Chiapas, where extensive new track construction and station development occurred during this period. Additional pockets of increased accessibility are observable in other regions, often around existing junctions, upgraded yards, or other major investment projects. These include the Inter-Oceanic Corridor of the Isthmus of Tehuantepec, spanning the states of Oaxaca and Veracruz; the Mexico City–Toluca Interurban Train in the central plateau; improvements in rail access to the Port of Guaymas along the Gulf of California in Sonora;

and the Patrick J. Ottensmeyer International Bridge, linking Nuevo Laredo, Tamaulipas, with Laredo, Texas.

Figure 3 here
---

c. Economic establishments

To capture the local economic structure and variation in productive activity, establishment-level information from INEGI's National Statistical Directory of Economic Units (DENUE) is also incorporated. The DENUE provides updated identification, location, and economic activity data for all active establishments in Mexico, excluding agricultural production units, mobile establishments, and selected regulated activities (INEGI, 2025). It includes information on commercial name, economic activity classified under the North American Industry Classification System (NAICS) 2023, employment size categories, and precise georeferenced coordinates. For each AGEB, annual counts of economic establishments are computed by intersecting establishment coordinates with AGEB polygons. Three key sectors are considered: manufacturing ($manuf_{it}$), construction ($const_{it}$), and transportation and warehousing ($trans_{it}$). Because the DENUE excludes mobile economic units and establishments without a fixed physical location, and because rural establishments may share a locality centroid (INEGI, 2025), this measures primarily capture formal and semi-formal fixed-location economic activity. As before, IHS transformations of these variables are used in the econometric analysis.

d. Road network

Lastly, to account for concurrent expansions of road infrastructure, annual geospatial layers of INEGI's National Road Network (RNC) for the period 2016–2024 were also

processed (INEGI, 2026b). The RNC is a high-resolution national transportation network modeled according to the international ISO 14825:2011 (GDF 5.0) standard. It integrates federal and state highways, urban and rural streets, rustic and unpaved roads, multimodal transport connections (ports, airports, ferry links), as well as logistics facilities and service infrastructure. The analysis here uses the vial (polyline) layer, which represents the topological structure of Mexico's road network. Each observation corresponds to a road segment defined between two geometric vertices. Polylines were decomposed into great-circle segments, and the length of each segment was computed using the Haversine formula. Summing across these yields the physical length for each road segment s:

$$road_km_s = \sum_{j=2}^{n_s} Haversine\left(x_{j-1}, y_{j-1}; x_j, y_j\right) \quad (3)$$

To spatially attribute road infrastructure to AGEBs, the centroid of each road segment was overlayed onto the AGEB polygons using point-in-polygon matching. Thus, for each AGEB i and year t, total road length was computed as:

$$road_{it} = \sum_{s \in S(i,t)} road_km_s \quad (4)$$

where $S(i,t)$ is the set of road segments whose centroids fall within AGEB i in year t. This measure captures annual road intensity at the AGEB level, which is also IHS-transformed and incorporated as a time-varying covariate.

Table 3 reports summary statistics for the variables used in the analysis, distinguishing between municipalities along the Tren Maya corridor and the rest of the country. On average, AGEBs in Tren Maya municipalities exhibit higher levels of night-time luminosity and lower rail accessibility than AGEBs elsewhere (i.e., longer distances to railway tracks and functional O-D rail points, as well as higher values of the accessibility

index $rail_{it}$). In terms of local economic structure, Tren Maya AGEBs have less manufacturing and transport & warehousing establishments, but slightly higher numbers of construction establishments and kilometers of road. Overall, the statistics unveil important heterogeneity between AGEBs in municipalities crossed by the Tren Maya alignment, and those located elsewhere in the country.

Table 3 here

III. EMPIRICAL STRATEGY

The empirical approach in this study exploits the staggered, spatially concentrated implementation of the Tren Maya railway across the southern states of Campeche, Yucatán, Quintana Roo, Tabasco, and Chiapas. Following the identification strategies of Donaldson (2018) and Faber (2014), changes in proximity to major infrastructure are interpreted as plausibly exogenous to short-term AGEB-level economic patterns, as investment decisions are centralized and not based on local growth dynamics. An additional feature reinforcing this interpretation is that a substantial share of the corridor follows pre-existing rights of way, including historical railway alignments, highways, and utility easements established decades earlier. As a result, much of the spatial configuration of the project reflects inherited infrastructure layouts rather than responses to recent economic trends. Because each municipality contains multiple AGEBs that share common local governance, infrastructure, and economic conditions, observations within the same municipality are likely to display spatial correlation. Therefore, the econometric analysis clusters standard errors at the municipal level (Colin Cameron and Miller, 2015; Abadie *et al.*, 2022).

a. TWFE model

The first part of the analysis is a two-way fixed-effects (TWFE) specification that exploits panel variation across AGEBs over the period 2016–2024. The objective is to assess how changes in railway accessibility are associated with local economic activity, proxied by IHS-transformed night-time light density. The baseline model is:

$$luminosity_{it} = \beta z_{it} + \gamma \mathbb{X}_{it} + \alpha_i + \delta_t + \sum_s \phi_s trend_{st} + \varepsilon_{it} \qquad (5)$$

where $luminosity_{it}$ denotes night-time light density per square kilometer in AGEB i at year t; $\mathbb{X}_{it}$ is a vector of IHS-transformed covariates including the number of manufacturing ($manuf_{it}$), construction ($const_{it}$), and transportation & warehousing ($trans_{it}$) establishments, as well as road infrastructure ($road_{it}$); α_i are AGEB fixed effects, absorbing all time-invariant local characteristics; δ_t are year fixed effects, accounting for national-level shocks; $trend_{st}$ is a set of 32 state-specific linear time trends; and ε_{it} is an error term clustered at the municipal level. Railway accessibility z_{it} is alternatively measured using the IHS transformations of the geodesic distance to the nearest rail track $dist_track_{it}$, the geodesic distance to the nearest functional rail origin–destination node $dist_od_{it}$, and the composite accessibility index derived from principal component analysis of the multiple distance measures, $rail_{it}$. In the first two cases, the coefficient β can be interpreted as the elasticity of luminosity with respect to rail distance, whereas in the index-based specification it captures the semi-elasticity of luminosity with respect to changes in overall rail accessibility. Table 4 reports the TWFE estimates. Across all specifications, the coefficient on railway accessibility is negative, indicating that

reductions in distance to rail infrastructure –or improvements in overall rail accessibility– are associated with higher levels of night-time luminosity.

Table 4 here

The magnitude and statistical significance of the estimates increase when using the origin-destination distance $dist_od_{it}$ or the accessibility index $rail_{it}$, and they remain stable when controlling for local economic structure and road infrastructure. These estimates suggest that improvements in rail accessibility are systematically correlated with increases in local economic activity, as captured by satellite-based measures of night-time light density per square kilometer, even after controlling for local production structure, road infrastructure, and unobserved time-invariant heterogeneity. For instance, the results in columns (3) and (4) show that a 10 percent reduction in the distance to the nearest functional rail origin-destination point is associated with an increase of approximately 0.19 to 0.21 percent in $luminosity_{it}$. When accessibility is summarized using the PCA-based rail accessibility index, the estimated coefficients capture the effect of a one-unit improvement in overall rail accessibility. Thus, the results in columns (5) and (6) indicate that a one-point increase in the rail accessibility index is associated with a 2.3 to 2.7 percent increase in $luminosity_{it}$, depending on the inclusion of controls. Overall, the TWFE results indicate a negative relationship between rail distance and night-time luminosity, and hence a positive relationship between rail accessibility and economic activity.

b. Event-study design

To characterize the dynamic effects of rail infrastructure expansion on local economic activity through luminosity, this part of the analysis implements an event-study design based on the difference-in-differences estimator proposed by Callaway and Sant'Anna (2021). This approach allows treatment effects to vary over time and across cohorts, relaxes the restrictive assumptions embedded in traditional two-way fixed-effects models, and provides a transparent assessment of pre-treatment trends. The empirical strategy exploits the gradual implementation of the Tren Maya project, which as mentioned above was announced in 2018, entered construction phase in 2020, and began operations on 15 December 2023. AGEBs exposed to the project are compared to appropriate control groups that were never treated, under alternative treatment definitions described below. Let $t_0 = 2018$ denote the first year of treatment. The baseline outcome equation is:

$$luminosity_{it} = luminosity_{it}(0) + \sum_{k \neq -1} 1\{t - t_0 = k\} \cdot ATT_k + \varepsilon_{it} \quad (6)$$

where $luminosity_{it}$ is the IHS transformation of the night-time light density per square kilometer, ATT_k denotes the average treatment effect on the treated at relative time k, and untreated potential outcomes are identified using never-treated AGEBs. Standard errors are clustered at the municipality level. Table 5 reports event-study estimates under six alternative treatment-control configurations, designed to progressively explore spatial heterogeneity in exposure to the Tren Maya. Figure 4 complements these results by visualizing the corresponding dynamic average treatment effects.

Table 5 here

Figure 4 here

The specifications are ordered from broader to more spatially precise definitions of treatment, allowing the analysis to move from municipality-level exposure and national-level contrast to a more localized proximity-based exposure. Columns (1) to (3) define treatment at the municipality level, assigning treated status to all AGEBs located within municipalities crossed by the Tren Maya alignment. Column (1) compares these treated AGEBs with never-treated AGEBs in the rest of the country (RoC) and excludes time-varying controls. While this specification provides a transparent benchmark, the estimates reveal a statistically significant pre-treatment coefficient, indicating that the unconditional parallel trends assumption is violated. In this specification, treated AGEBs were already following different luminosity trajectories prior to the announcement of the project. Column (2) introduces controls for local economic structure and road infrastructure to attempt identification under the assumption of conditional parallel trends. However, the pre-treatment coefficient remains statistically different from zero. This result suggests that differences in pre-treatment trends are not fully explained by observable characteristics, and that municipality-level treatment definitions might remain too broad to isolate the effects of the Tren Maya from regional dynamics. Column (3) restricts the control group to never-treated AGEBs located in other municipalities of the southeastern states that were not crossed by the Tren Maya alignment (RoSE). By comparing treated and control units within the same macro-region, this specification reduces concerns about differential regional trends. The pre-treatment coefficient becomes smaller and statistically insignificant, providing stronger support for the parallel trends assumption. However, post-treatment effects are neither consistent in sign nor in statistical significance. As shown in Figure 4 panel (3), their pattern suggests that, relative to comparable southeastern areas,

any luminosity gains in Tren Maya municipalities may be concentrated in a narrow window during the construction phase, rather than exhibiting a sustained post-treatment divergence.

Columns (4) to (6) adopt a more spatially targeted definition of treatment based on proximity to the infrastructure itself. Treated units are now AGEBs whose centroids fall within a 15-km buffer around the Tren Maya alignment, as depicted in Figure 5. Column (4) compares these buffer AGEBs with never-treated AGEBs in the rest of the country. The pre-treatment coefficient is small and statistically indistinguishable from zero, providing no evidence of differential trends prior to the announcement of the project. Following the start of construction, the estimates display a short-lived decline around 2020–2021, consistent with temporary disruption effects of the Covid-19 pandemic. From 2022 onward, post-treatment coefficients turn positive and statistically significant. The mean post-treatment ATT implies that AGEBs located within the 15-km buffer around the Tren Maya experienced, on average, an increase of approximately 4.1 percent in night-time light density per square kilometer relative to untreated areas. Column (5) further restricts the control group to AGEBs located in southeastern states but outside the 15-km buffer around the Tren Maya corridor. Under this specification, the pre-treatment coefficient remains statistically indistinguishable from zero, reinforcing the credibility of the parallel trends assumption in a geographically comparable sample. Some of the post-treatment effects are of similar magnitude to those obtained in column (4) but display a smoother and more stable dynamic profile. As illustrated in Figure 4 panel (5), estimated annual treatment effects remain consistently above 0.05 in the post-pandemic period, suggesting a persistent increase in night-time luminosity in AGEBs exposed to the corridor relative to other southeastern areas not directly affected by the project. Finally, column (6) implements the

most spatially stringent comparison by contrasting AGEBs whose centroids fall within the 15-km buffer around the Tren Maya alignment with those located within the same municipalities crossed by this buffer, but whose centroids fall outside of it (RoB). Under this specification, the pre-treatment coefficient remains close to zero and statistically insignificant, providing support for the unconditional parallel trends assumption. Treatment effects are positive and statistically significant in 2019 and 2022–2024. The mean post-treatment ATT implies that AGEBs located within the 15-km buffer around the Tren Maya experienced, on average, an increase of 4.6 percent in night-time light density per square kilometer relative to nearby AGEBs that were not directly exposed to the corridor.

Across all these specifications, particularly those relying on the 15-km buffer treatment definition, the event-study profiles display three consistent patterns: The absence of differential pre-trends; a temporary decline in luminosity around 2020–2021, consistent with pandemic-related disruptions; and a sustained positive response beginning in 2022 and intensifying through the corridor's entry into operation in 2024.

Appendix Tables A1 and A2 report a set of robustness checks that further qualify and strengthen the main findings of the analysis. Table A1 explores alternative definitions of spatial exposure by varying the buffer radius around the Tren Maya alignment. When narrower buffers are used (5 km and 10 km), the parallel-trends assumption fails to hold, both unconditionally and conditionally on controls. This likely reflects the fact that AGEBs located extremely close to the corridor differ systematically from more distant areas even prior to construction, for instance due to pre-existing tourism activity, urbanization, or site-selection criteria related to the project itself. In contrast, when a wider buffer (20 km) is used, the unconditional parallel-trends assumption holds, and the estimated mean post-

treatment ATTs are smaller but also statistically significant. Table A2 examines sensitivity to the timing of treatment by redefining $t_0 = 2020$, when construction of the Tren Maya corridor effectively began. Under this alternative specification, the assumption of parallel trends is harder to sustain, and estimated treatment effects in the post-2020 period are dominated by large and statistically significant negative coefficients in 2020 and 2021. This reflects the profound economic disruptions associated with the Covid-19 pandemic, making it difficult to disentangle the impact of the Tren Maya from contemporaneous pandemic-related declines in economic activity.

In sum, these findings provide evidence that improvements in railway accessibility associated with the implementation of the Tren Maya corridor are followed by increases in luminosity. The dynamic patterns indicate that these effects materialize gradually, intensify towards the completion of construction, and are strongest for AGEBs located closest to the new railway infrastructure.

IV. LUMINOSITY-BASED MEASURES OF LOCAL ECONOMIC ACTIVITY

Measuring economic activity at a fine spatial scale poses significant empirical challenges, particularly in settings where official economic statistics are infrequent, highly aggregated, or unavailable below certain administrative levels. While national accounts provide reliable measures of aggregate output, they offer limited insight into localized economic dynamics, which are central to understanding the spatial effects of transport infrastructure investments.

The use of night-time luminosity in this circumstances is grounded in the seminal contribution of Henderson *et al.* (2012), who demonstrate that changes in this measure are

strongly correlated with changes in real economic activity. Their analysis shows that satellite-based luminosity data can complement conventional statistics by providing consistent, high-frequency, and spatially disaggregated information when subnational economic data are limited or subject to measurement error. A central insight of this literature is that night-time lights are most informative when used to capture relative changes in economic activity over time, rather than to approximate absolute levels of income or output. Ghosh *et al.* (2010) also emphasize the value of night-time lights for analyzing the global and subnational distribution of economic activity. By exploiting high-resolution satellite imagery, they document how artificial lighting captures patterns of economic concentration, urbanization, and spatial inequality across and within countries.

From an economic perspective, night-time luminosity reflects a composite outcome of productive, commercial, and residential activity. Increases in light density are associated with greater use of infrastructure, higher levels of economic interaction, and intensified service provision, all of which accompany economic expansion. The key strength of this proxy lies in its ability to capture economic dynamics consistently across space, even in the absence of local economic statistics. These properties make satellite-based luminosity data especially well-suited for evaluating the localized impacts of transport infrastructure.

Transport investments affect economic outcomes through changes in accessibility and connectivity, reducing transport and trade costs and generating spatially heterogeneous responses that may not be immediately reflected in aggregate indicators. Studies such as Storeygard (2016) and Mitnik *et al.* (2018) exploit these features to assess the economic effects of transport-related investments, showing that night-time luminosity provides a useful proxy for detecting localized effects of infrastructure projects that are often obscured

in conventional statistics. This line of work complements structural analyses such as Donaldson (2018), who shows that large-scale transport infrastructure, including railroads, can substantially increase real income by integrating markets and lowering trade costs.

Despite its advantages, luminosity is an imperfect proxy for economic activity and presents several well-documented limitations. Light intensity may saturate in densely urbanized areas, underrepresent informal or low-electricity activities, and exhibit a mass of zero observations in sparsely populated regions. Consistent with Henderson *et al.* (2012) and similar to Mitnik *et al.* (2018), this study addresses these concerns by focusing on within-location variation over time, applying the inverse hyperbolic sine transformation to accommodate zero values (Pence, 2006), and employing fixed-effects specifications that control for time-invariant differences across locations. Accordingly, night-time luminosity is interpreted as an indicator of relative changes in local economic activity and its spatial distribution, rather than as a direct measure of output or income levels. This interpretation is particularly appropriate for this case, given that AGEB-level economic statistics are unavailable, whereas large-scale transport investments such as the Tren Maya corridor are expected to generate localized and spatially heterogeneous economic effects.

a. Interpretation of changes in luminosity

To provide an economic interpretation of the effects estimated from the event-study design, this section draws on benchmark elasticities between economic activity and luminosity previously reported in the literature. Using a global panel of countries, Henderson *et al.* (2012) estimate elasticities of real GDP with respect to night-time lights in the range of 0.28 to 0.32, depending on the specification and time horizon. These estimates

capture aggregate growth relationships and provide an upper bound for interpreting changes in luminosity. On the other hand, Mitnik *et al.* (2018) estimate substantially lower elasticities in a highly localized setting, using a long time series for Haiti. Their results suggest values in the range of 0.06 to 0.08, reflecting that at finer spatial resolutions and in lower-income contexts, changes in luminosity may capture only a subset of economic activity or may be affected by measurement noise, saturation, or informal production.

Taken together, these studies define a plausible range of elasticities linking night-time luminosity to real GDP, with a lower-bound value of 0.06 and an upper-bound value of 0.32, as summarized in Table 6. To complement these benchmarks, this study estimates Mexico-specific elasticities using a panel of state-level real GDP at constant 2018 prices and the night-time luminosity measure aggregated from the AGEB-level data. Fixed-effects regressions with state and year effects are estimated under alternative specifications with and without the additional controls for state-level economic structure and road infrastructure. Across all specifications, the estimated elasticities fall within the benchmark range established by the literature.

Table 6 here

Thus, using these reference values, the ATTs reported in Table 5 can be translated into implied changes in local economic activity. For example, the estimated average post-treatment increase in luminosity of 1.0% for AGEBs located in Tren Maya municipalities (column 3) would correspond to an increase in local economic activity ranging from 0.06% under the lower-bound elasticity to 0.32% under the upper-bound elasticity. For AGEBs within a 15-km buffer around the Tren Maya alignment, the estimated luminosity effects

are larger and statistically significant, yielding implied economic gains between 0.20% under the lower-bound elasticity and 1.47% under the upper-bound elasticity (columns 4–6). When the benchmark interval is restricted to the elasticities estimated using 2016–2024 Mexican state-level data, the implied effects on economic activity range between 0.59% and 0.92%. These values suggest that the economic effects associated with improved accessibility induced by the Tren Maya rail corridor are meaningful, particularly in areas located closer to the rail alignment. Importantly, these calculations are intended to convey an order of magnitude of the implied economic effects across the alternative empirical specifications considered in the analysis.

V. SPATIAL HETEROGENEITY AND STATE-LEVEL EFFECTS

This section explores the spatial heterogeneity of the economic impacts of the Tren Maya by disaggregating the event-study analysis at the state level. While the previous sections document average effects across the entire corridor, there are strong reasons to expect substantial variation across space, given the heterogeneity in baseline economic conditions, sectoral composition, urbanization, and exposure to tourism across southeastern Mexico. To capture these differences, the event-study model is re-estimated separately for each of the five states crossed by the corridor: Campeche, Chiapas, Quintana Roo, Tabasco, and Yucatán. The empirical strategy adopts a more targeted definition of treatment. Treated units are now AGEBs whose centroids lie within a 2.5-km buffer around the Tren Maya alignment, while the control group consists of never-treated AGEBs located in the same state. This within-state comparison allows to isolate highly localized treatment effects while controlling for state-specific trends and unobserved heterogeneity. Depending on the

state, the same covariates previously used to capture local economic structure and road infrastructure are included when required to satisfy the parallel-trends assumption.

Table 7 reports dynamic ATTs for each state. Several salient patterns emerge. First, the results reveal substantial heterogeneity in both the magnitude and timing of the effects across states. Campeche, Chiapas, and Quintana Roo exhibit positive and statistically significant post-treatment effects toward the later stages of the construction period. In Campeche, ATTs become positive and statistically significant in 2023 and reaches 0.127 in 2024, when the train begins to operate. Chiapas displays the largest effects among all states, with post-treatment ATTs exceeding 0.5 by 2024, pointing to strong localized impacts, likely associated with construction intensity and complementary investments along the southern segment of the project. Quintana Roo also shows a positive response under conditional parallel trends, with statistically significant effects emerging in 2023 and intensifying in 2024.

Table 7 here

Second, Yucatán presents a more muted response. The pre-treatment ATT is positive and statistically significant, and the pre-trends test rejects the null of no differential pre-trends even when covariates are included. Moreover, all post-treatment ATTs are positive but statistically indistinguishable from zero throughout. This implies that in the case of this state there is no evidence of localized luminosity gains attributable to the corridor. One plausible interpretation is that large parts of the state were already experiencing a distinct growth trajectory prior to the project, driven in part by sustained expansion in residential

development, tourism, and related services, which may mask or dominate any incremental effects associated with the new rail infrastructure.

Third, Tabasco stands out as a negative outlier. Across all post-treatment periods, estimated ATTs are negative and statistically significant, reaching -0.403 by 2024. This contrasts sharply with the positive effects observed in other states and suggests that, in this case, construction-related disruptions, environmental externalities, land-use reorganization, or displacement effects may have outweighed short-run economic benefits. Appendix Figure A1 shows that AGEBs located within the buffer experienced a sharp decline in luminosity beginning in 2018, well before the formal start of construction, pointing to anticipatory adjustment costs. Although luminosity partially recovers after 2020, treated areas do not regain their pre-project relative position, resulting in persistently negative treatment effects throughout the construction phase.

The event-study profiles displayed in Figure 6 complement these findings by illustrating the dynamic evolution of treatment effects over time. With the exception of Yucatán, pre-treatment coefficients are close to zero and statistically insignificant, lending support to the plausibility of the parallel-trends assumption. Following the onset of construction, most states exhibit a temporary downturn around 2020-2021, consistent with the effects of pandemic-related disruptions. From 2022 onward, positive effects materialize and strengthen in Campeche, Chiapas, and Quintana Roo, while Yucatán shows no significant gains, and Tabasco continues to display persistent negative responses.

Figure 6 here

Overall, these results confirm the localized and heterogeneous nature of the economic impacts of the Tren Maya. Even within a relatively compact geographic region, the project has generated contrasting outcomes, ranging from large positive effects in Chiapas to sustained negative impacts in Tabasco. These differences likely reflect interactions between the new infrastructure, pre-existing economic structures, sectoral specialization, environmental conditions, and the spatial distribution of complementary investments. More broadly, the findings suggest that large transport investments do not yield uniform local benefits and that transitional adjustment costs can be substantial, so that their economic consequences depend critically on regional context.

VI. CONCLUSIONS

This paper examined the local economic effects of the Tren Maya railway project using satellite-based night-time luminosity data combined with detailed geospatial information on Mexico's rail network. Exploiting spatial and temporal variation in proximity to the new infrastructure at the AGEB level for the period 2016–2024, the analysis provides new evidence on how large-scale rail investments affect localized economic activity.

A relevant feature of the Tren Maya is that both its planning and spatial configuration were largely determined through a centralized federal decision-making process, rather than by local economic conditions. Moreover, a substantial share of the alignment reuses historical railway corridors and long-established rights of way associated with functional highways and electricity transmission lines. This reliance on pre-existing infrastructure layouts implies that much of the spatial configuration of the project reflects historical and engineering constraints rather than contemporaneous patterns of economic growth, which

strengthens the plausibility of the identifying assumptions of the empirical strategy, and the causal interpretation of the estimated effects.

Three main conclusions emerge from the empirical results. First, improvements in rail accessibility are correlated with increases in night-time luminosity. Two-way fixed-effects estimates show that reductions in distance to railway infrastructure and improvements in a composite accessibility index are associated with higher levels of local light density, even after controlling for local economic structure, road infrastructure, and unobserved time-invariant heterogeneity. These findings are consistent with a growing literature that documents positive but spatially heterogeneous economic responses to transport infrastructure investments.

Second, event-study estimates reveal that the economic effects derived from the implementation of the Tren Maya in the Mexican southeast are highly localized and depend on how treatment exposure is defined. Specifications based on broad, municipality-level treatment definitions fail to satisfy the parallel-trends assumption and yield unstable post-treatment effects. In contrast, when treatment is defined using spatial buffers around the railway alignment –particularly within a 15-km radius– the identifying assumptions are more credible, and the estimated effects are both economically meaningful and statistically robust. AGEBs located close to the corridor experienced sustained increases in luminosity beginning in 2022, intensifying through the onset of railway operations in 2024. This pattern indicates that the impacts of large-scale transport infrastructure project are unlikely to diffuse evenly across administrative boundaries. Interpreting these results through benchmark elasticities linking night-time luminosity to real economic activity suggests that the implied effects, while modest in aggregate terms, are economically meaningful at the

local level. For areas directly exposed to the corridor, and depending on the choice of control group, the estimated increases in luminosity translate into gains in local economic activity ranging from 0.20% to 1.47% (or from 0.59% to 0.92% when the benchmark interval is restricted to the elasticities estimated in this study using Mexican data for the 2016–2024 period only).

Third, the dynamic profiles reveal substantial heterogeneity in both the magnitude and timing of impacts across states. Disaggregated event-study estimates show sizable and statistically significant positive effects in Chiapas, Campeche, and Quintana Roo, particularly toward the later stages of construction and early operation, which is consistent with strong localized responses to infrastructure investment and complementary development activities. In contrast, Yucatán exhibits no statistically significant post-treatment gains and displays evidence of differential pre-trends, suggesting that pre-existing growth dynamics –most likely linked to residential development, tourism, and service-sector expansion– may dominate any incremental effects of the new rail infrastructure. Most strikingly, Tabasco experiences a persistent and statistically significant decline in luminosity throughout the construction period, pointing to the potential importance of construction-related disruptions, environmental externalities, or displacement effects. Together, these findings suggest that even within a relatively compact geographic region, the economic consequences of major transport investments can vary sharply, reflecting interactions between infrastructure, local economic structures, sectoral specialization, and institutional context.

From a methodological perspective, this paper reinforces the value of combining satellite-based data with geospatial measures of infrastructure accessibility to study

localized economic effects in settings where conventional statistics are unavailable or insufficiently disaggregated. At the same time, the use of night-time luminosity as a proxy entails well-known limitations, as it does not capture all dimensions of economic performance, including informal activity, sectoral composition, or welfare outcomes.

From a policy point of view, the results suggest that while flagship infrastructure projects such as the Tren Maya can stimulate local economic activity, their effects are geographically concentrated and unlikely to propagate automatically and evenly to surrounding areas. This implies that complementary policies such as land-use planning, local business development, and connectivity to secondary transport networks, may be necessary to translate localized accessibility gains into more diffuse and inclusive regional development. As the Tren Maya project matures and additional post-operation data become available, future research should assess whether the observed effects reflect temporary construction-related dynamics or evolve into sustained long-term growth.

Finally, it is important to keep in mind that the analysis presented in this paper captures only one dimension of the overall impact of the Tren Maya project. Changes in night-time luminosity provide a proxy for local economic activity, but they do not account for other relevant dimensions of welfare. In particular, the project has generated significant environmental externalities, including ecosystem fragmentation, biodiversity loss, and pressures on ecologically sensitive areas of the Yucatán Peninsula. These effects remain unmeasured in the present framework. A holistic evaluation would therefore require combining the localized economic gains documented here with equally rigorous estimates of environmental and social costs.

Acknowledgements

The author is grateful to Susana Marín Soots and Ariel Kessel Akerman for their valuable advice and technical support during the preparation of this paper. The author also thanks Oscar Mitnik and Luis Eduardo Quintero Escobar, for insightful and constructive feedback that substantially improved the quality of this work. The author acknowledges the use of artificial intelligence–based tools to assist with language editing and stylistic improvements during the preparation of this manuscript. All substantive content, analyses, interpretations, and conclusions are the sole responsibility of the author.

References

Abadie, A., Athey, S., Imbens, G. and Wooldridge, J. (2022) "When Should You Adjust Standard Errors for Clustering?," *The Quarterly Journal of Economics*, 138(1), pp. 1–35. Available at: https://doi.org/10.1093/qje/qjac038.

Acevedo, J., Sánchez, D., Romero, R. and Valdéz, O. (2025) "El impacto social y económico por el Tren Maya en 25 años, en el sureste mexicano," *Ciencia Latina Revista Científica Multidisciplinar*, 9(1), pp. 12959–12978. Available at: https://doi.org/10.37811/CL_RCM.V9I1.16913.

Alhassan, J.A.K. and Anciaes, P. (2025) "Public transport investments as generators of economic and social activity," *Journal of Transport & Health*, 41, p. 101989. Available at: https://doi.org/10.1016/j.jth.2025.101989.

ARTF (2026) *Red Ferroviaria Nacional*, *Agencia Reguladora del Transporte Ferroviario, Gobierno de México*. Available at: https://www.gob.mx/artf/documentos/mapas-del-sistema-ferroviario-mexicano (Accessed: January 28, 2026).

Banerjee, A., Duflo, E. and Qian, N. (2020) "On the road: Access to transportation infrastructure and economic growth in China," *Journal of Development Economics*, 145. Available at: https://doi.org/10.1016/j.jdeveco.2020.102442.

Brajša-Žganec, A., Merkaš, M. and Šverko, I. (2011) "Quality of Life and Leisure Activities: How do Leisure Activities Contribute to Subjective Well-Being?," *Social Indicators Research*, 102(1), pp. 81–91. Available at: https://doi.org/10.1007/s11205-010-9724-2.

Calderon, C. and Serven, L. (2010) "Infrastructure and Economic Development in Sub-Saharan Africa," *Journal of African Economies*, 19(Supplement 1), pp. i13–i87. Available at: https://doi.org/10.1093/jae/ejp022.

Callaway, B. and Sant'Anna, P.H.C. (2021) "Difference-in-Differences with multiple time periods," *Journal of Econometrics*, 225(2), pp. 200–230. Available at: https://doi.org/10.1016/j.jeconom.2020.12.001.

Çelik, A.K., Yalçınkaya, Ö. and Kutlu, M. (2025) "The causal relationship between air transport and economic growth: Evidence from top ten countries with the largest air transport volume," *Transport Policy*, 162, pp. 521–532. Available at: https://doi.org/10.1016/J.TRANPOL.2025.01.002.

Colin Cameron, A. and Miller, D.L. (2015) "A Practitioner's Guide to Cluster-Robust Inference," *Journal of Human Resources*, 50(2), pp. 317–372. Available at: https://doi.org/10.3368/jhr.50.2.317.

Cruz, R.I.G., Torres, M.Y.C. and López, J.A.S. (2023) "Environmental, social and economic impact of the mayan train on indigenous peoples in southeastern Mexico," *Nexo Revista Científica*, 36(06), pp. 839–853. Available at: https://doi.org/10.5377/NEXO.V36I06.17440.

DOF (2019) *Plan Nacional de Desarrollo 2019-2024*, *Diario Oficial de la Federación,Presidencia de la República, Estados Unidos Mexicanos*. Available at: https://www.dof.gob.mx/nota_detalle.php?codigo=5565599&fecha=12/07/2019#gsc.tab=0 (Accessed: January 7, 2026).

Donaldson, D. (2018) "Railroads of the Raj: Estimating the Impact of Transportation Infrastructure," *American Economic Review*, 108(4–5), pp. 899–934. Available at: https://doi.org/10.1257/AER.20101199.

Duranton, G. and Puga, D. (2023) "Urban Growth and Its Aggregate Implications," *Econometrica*, 91(6), pp. 2219–2259. Available at: https://doi.org/10.3982/ECTA17936.

Elvidge, C.D., Zhizhin, M., Ghosh, T., Hsu, F.C. and Taneja, J. (2021) "Annual Time Series of Global VIIRS Nighttime Lights Derived from Monthly Averages: 2012 to 2019," *Remote Sensing 2021, Vol. 13, Page 922*, 13(5), p. 922. Available at: https://doi.org/10.3390/RS13050922.

Faber, B. (2014) "Trade Integration, Market Size, and Industrialization: Evidence from China's National Trunk Highway System," *The Review of Economic Studies*, 81(3), pp. 1046–1070. Available at: https://doi.org/10.1093/RESTUD/RDU010.

Fogel, R.W. (1964) *Railroads and American Economic Growth: Essays in Econometric History*. Baltimore: The Johns Hopkins Press.

FONATUR (2020) *Programa Institucional 2020-2024 de Fonatur Tren Maya, S.A. de C.V.* Mexico City.

Ghosh, T., Powell, R., Elvidge, C.D., Baugh, K., Sutton, P. and Anderso, S. (2010) "Shedding Light on the Global Distribution of Economic Activity," *The Open Geography Journal*, 3, pp. 147–160.

González Moreno, J.O., Cruz González, G. and Arroyo Osorno, J.A. (2024) *Impacto socioeconómico territorial de las obras ferroviarias más importantes del sexenio 2019-2024*. 859. Querétaro, México.

Gonzalez-Navarro, M. and Turner, M.A. (2018) "Subways and urban growth: Evidence from earth," *Journal of Urban Economics*, 108, pp. 85–106. Available at: https://doi.org/10.1016/J.JUE.2018.09.002.

Han, Z. and Li, H. (2022) "Transportation infrastructure and trade," *Japan and the World Economy*, 64. Available at: https://doi.org/10.1016/j.japwor.2022.101162.

Henderson, J.V., Storeygard, A. and Weil, D.N. (2012) "Measuring Economic Growth from Outer Space," *American Economic Review*, 102(2), pp. 994–1028. Available at: https://doi.org/10.1257/AER.102.2.994.

INEGI (2025) *Directorio Estadístico Nacional de Unidades Económicas: DENUE Interactivo 05/2025, Documento Metodológico*. Mexico City. Available at: www.inegi.org.mx.

INEGI (2026a) *Marco Geoestadístico*, *Instituto Nacional de Estadística y Geografía*. Available at: https://www.inegi.org.mx/temas/mg/ (Accessed: January 28, 2026).

INEGI (2026b) *Red Nacional de Caminos (RNC)*, *Instituto Nacional de Estadística y Geografía*. Available at: https://www.inegi.org.mx/programas/rnc/ (Accessed: January 28, 2026).

Jolliffe, I.T. (2002) *Principal Component Analysis*. 2nd ed. New York: Springer-Verlag (Springer Series in Statistics). Available at: https://doi.org/10.1007/B98835.

Krugman, P.R. (1980) "Scale Economies, Product Differentiation, and the Pattern of Trade," *American Economic Review*, 70, pp. 950–959.

Mitnik, O.A., Sanchez, R. and Yañez-Pagans, P. (2018) *Bright investments: Measuring the impact of transport infrastructure using luminosity data in Haiti*. Washington DC. Available at: http://www.iadb.org.

Monte, F., Redding, S.J. and Rossi-Hansberg, E. (2018) "Commuting, Migration, and Local Employment Elasticities," *American Economic Review*, 108(12), pp. 3855–3890. Available at: https://doi.org/10.1257/aer.20151507.

Moreno-Brid, J.C., Carpizo, J.E.P. and Bosch, J.R. (2009) "Economic development and social policies in Mexico," *Economy and Society*, pp. 154–176. Available at: https://doi.org/10.1080/03085140802560652.

Moreno-Brid, J.C. and Ros, J. (2009) *Development and Growth in the Mexican Economy*. Oxford University Press. Available at: https://doi.org/10.1093/acprof:oso/9780195371161.001.1.

Ouni, M., Mraihi, R., Mrad, S. and El Montasser, G. (2025) "Exploring the Dynamic Linkages Between Poverty, Transportation Infrastructure, Inclusive Growth and Technology: A Continent-Wise Comparison in Lower-Middle-Income Countries," *Journal of the Knowledge Economy 2025 16:5*, 16(5), pp. 16820–16869. Available at: https://doi.org/10.1007/S13132-024-02516-5.

Pence, K.M. (2006) *The Role of Wealth Transformations: An Application to Estimating the Effect of Tax Incentives on Saving*.

Pi, Y. and Wang, Y. (2025) "Transportation infrastructure, comparative advantage, and regional specialization: Evidence from China's high-speed railway network," *Transportation Research Part A: Policy and Practice*, 191, p. 104334. Available at: https://doi.org/10.1016/J.TRA.2024.104334.

Picard, R. (2019) “GEONEAR: Stata module to find nearest neighbors using geodetic distances,” *Statistical Software Components* [Preprint]. Available at: https://ideas.repec.org/c/boc/bocode/s457146.html (Accessed: November 9, 2025).

Scholl, L. *et al.* (2022) *Transporte para el desarrollo inclusivo:un camino para América Latina y el Caribe*. Available at: https://publications.iadb.org/publications/spanish/document/Transporte-para-el-desarrollo-inclusivo-un-camino-para-America-Latina-y-el-Caribe.pdf (Accessed: August 21, 2025).

Storeygard, A. (2016) “Farther on down the road: Transport costs, trade and urban growth in sub-Saharan Africa,” *Review of Economic Studies*, 83(3), pp. 1263–1295. Available at: https://doi.org/10.1093/restud/rdw020.

The World Bank (2007) *Annual World Bank Conference on Development Economics 2007, Global*. Edited by F. Bourguignon and B. Pleskovic. The World Bank. Available at: https://doi.org/10.1596/978-0-8213-6841-1.

Varghese, A.M. and Pradhan, R.P. (2025) “Transportation infrastructure and economic growth: Does there exist causality and spillover? A Systematic Review and Research Agenda,” *Transportation Research Procedia*, 82, pp. 2618–2632. Available at: https://doi.org/10.1016/J.TRPRO.2024.12.208.

Villarreal, M.A. and Fergusson, I.F. (2017) *The North American Free Trade Agreement (NAFTA)*. Available at: www.crs.gov.

FIGURES



Figure 1 The Tren Maya corridor

Notes: Author's own elaboration. Alignment of the Tren Maya railway corridor across southeastern Mexico, covering the states of Chiapas, Tabasco, Campeche, Yucatan, and Quintana Roo.

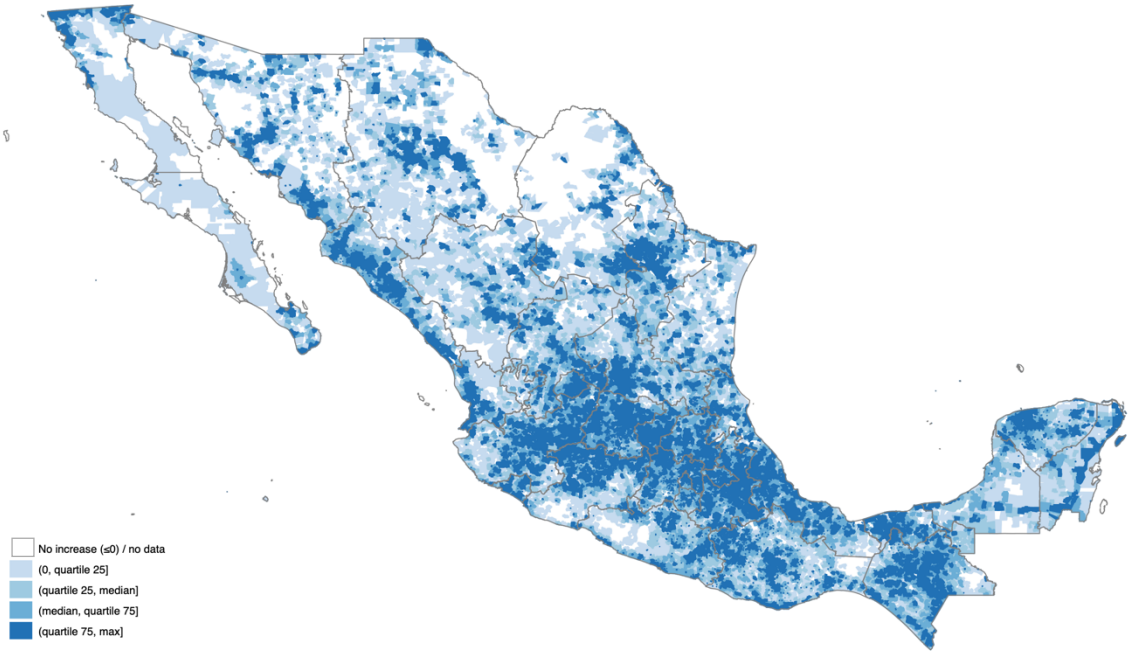


Figure 2 Increase in night-time luminosity, 2016–2024

Notes: Author's elaboration with data from the Visible Infrared Imaging Radiometer Suite (VIIRS) Day/Night Band "median masked" annual composites, produced by the Earth Observation Group at NOAA/NASA's National Polar-Orbiting Partnership–Suomi satellite (Elvidge *et al.*, 2021); and INEGI's 2024 geostatistical framework. White = no increase or missing data; progressively darker blue = progressively larger increase in luminosity.

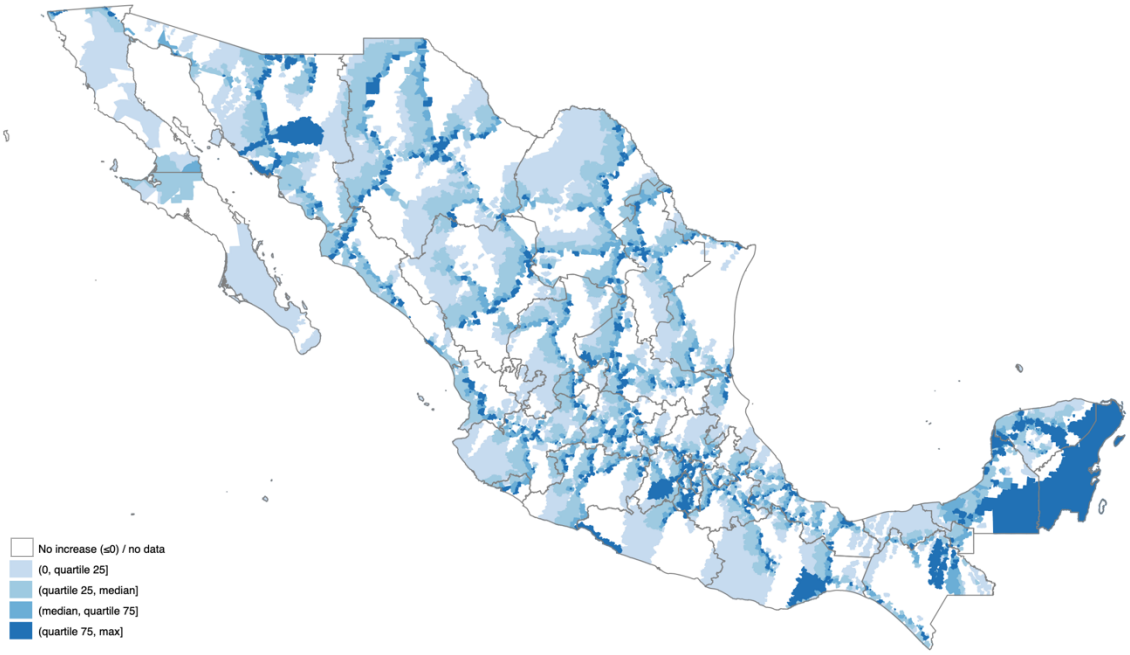
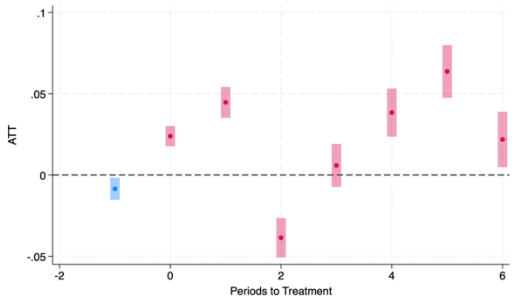
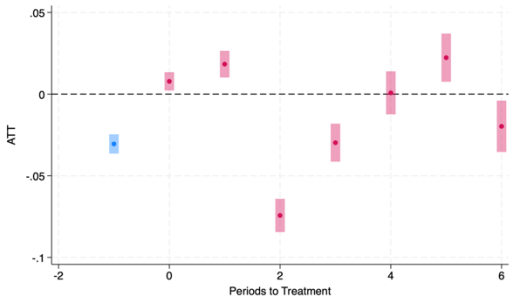


Figure 3 Increase in proximity to railway infrastructure, 2016–2024

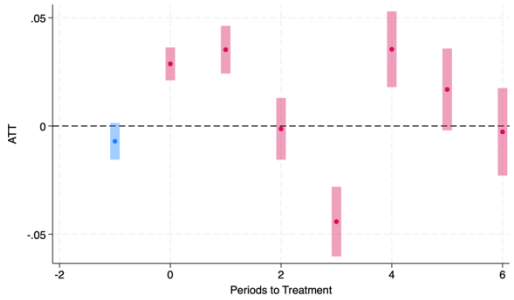
Notes: Author's elaboration with data from Mexico's Regulatory Agency for Rail Transport (ARTF) and INEGI's 2024 geostatistical framework. White = no increase in proximity or missing data; progressively darker blue = progressively larger increase in proximity.



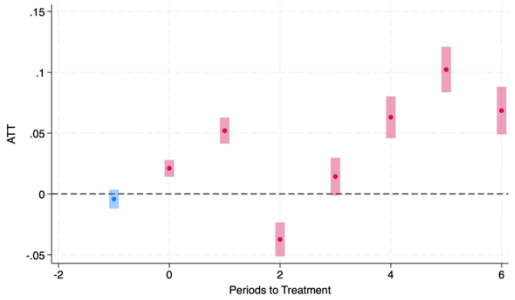
(1) AGEBs in Tren Maya municipalities vs Rest of the Country (no controls)



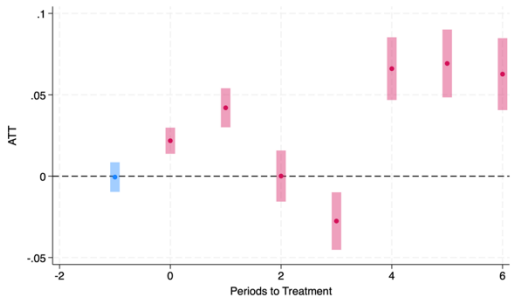
(2) AGEBs in Tren Maya municipalities vs Rest of the Country (with controls)



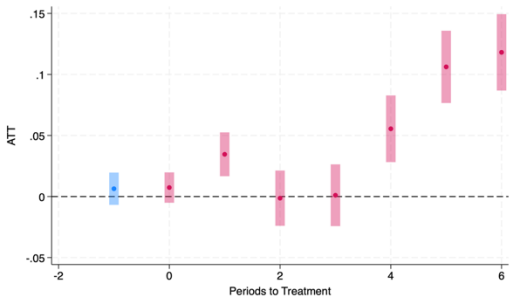
(3) AGEBs in Tren Maya municipalities vs Rest of Southeast (no controls)



(4) AGEBs with centroids within 15-km buffer around Tren Maya vs Rest of the Country (no controls)



(5) AGEBs with centroids within 15-km buffer around Tren Maya vs Rest of Southeast (no controls)



(6) AGEBs with centroids within 15-km buffer around Tren Maya vs AGEBs in same municipalities but outside buffer (no controls)

Figure 4 Dynamic treatment effects of the Tren Maya under alternative treatment definitions

Notes: Event-study estimates of the average treatment effect on the treated (ATT) using the Callaway and Sant'Anna (2021) difference-in-differences estimator with multiple time periods. Each panel corresponds to a different treatment definition, as described in Table 4. The horizontal axis measures periods relative to the first year of treatment (2018), and the vertical axis reports ATT estimates. Blue markers denote pre-treatment coefficients, while red markers denote post-treatment effects. Vertical bars represent 95% confidence intervals. Standard errors are clustered at the municipality level. The dashed horizontal line indicates zero effect.

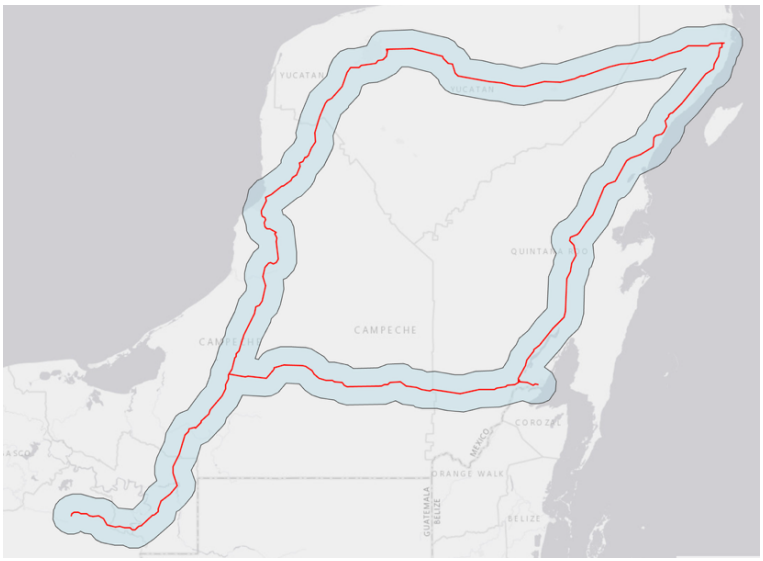


Figure 5 Tren Maya alignment and 15-km buffer used to define spatial treatment exposure in the baseline scenario

Notes: The red line depicts the official alignment of the Tren Maya rail corridor based on 2024 ARTF geospatial data. The shaded area corresponds to a 15-km geodesic buffer constructed around the rail alignment and used to define treated AGEBs in the event-study analyses. AGEBs whose centroids fall within the buffer are classified as treated, while AGEBs outside the buffer serve as potential control units depending on the specification.

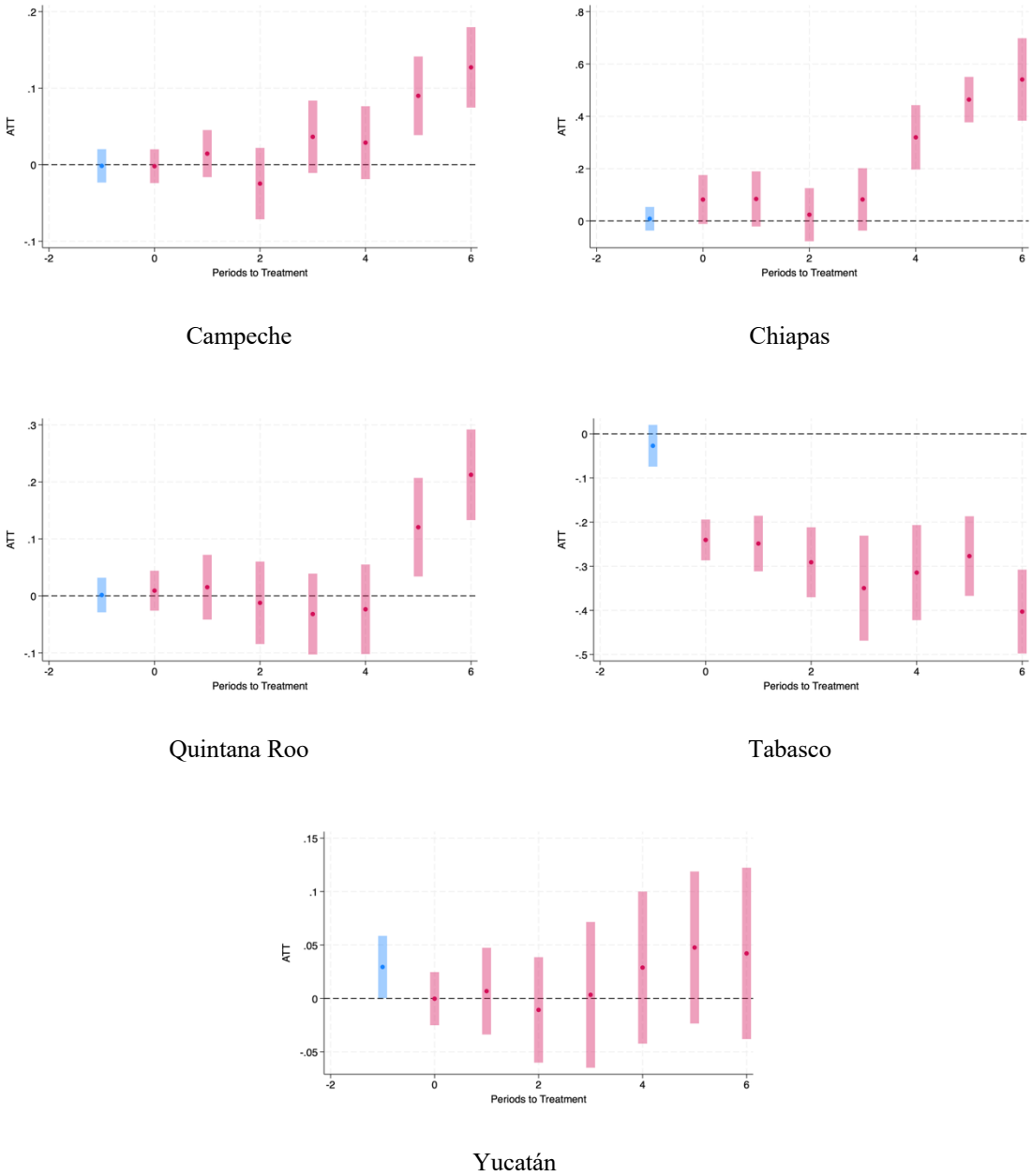


Figure 6 Spatial heterogeneity of the economic effects of the Tren Maya

Notes: Event-study estimates of the average treatment effect on the treated (ATT) using the Callaway and Sant'Anna (2021) difference-in-differences estimator with multiple time periods. Each panel corresponds to each of the southeastern Mexican states crossed by the Tren Maya alignment, as described in Table 6. The horizontal axis measures periods relative to the first year of treatment (2018), and the vertical axis reports ATT estimates. Blue markers denote pre-treatment coefficients, while red markers denote post-treatment effects. Vertical bars represent 95% confidence intervals. Standard errors are clustered at the municipality level. The dashed horizontal line indicates zero effect.

TABLES

Table 1 Pearson correlations among railway infrastructure variables

	$dist_track_{it}$	$dist_node_{it}$	$dist_struct_{it}$	$dist_od_{it}$	$dist_mark_{it}$
$dist_track_{it}$	1.000				
$dist_node_{it}$	0.847 *** [0.000]	1.000			
$dist_struct_{it}$	0.887 *** [0.000]	0.760 *** [0.000]	1.000		
$dist_od_{it}$	0.814 *** [0.000]	0.807 *** [0.000]	0.874 *** [0.000]	1.000	
$dist_mark_{it}$	0.893 *** [0.000]	0.774 *** [0.000]	0.958 *** [0.000]	0.854 *** [0.000]	1.000

Note: Pearson correlation coefficients. Significance levels: 0 '***' 0.001 '**' 0.01 '*' 0.05.

Table 2 Principal component analysis of IHS-transformed railway distance measures

Panel A: Eigenvalues and variance explained			
Component[a]	Eigenvalue	Proportion of Variance	Cumulative
PC1	4.090	0.818	0.818
PC2	0.493	0.099	0.917
PC3	0.271	0.054	0.971
PC4	0.097	0.019	0.990
PC5	0.049	0.010	1.000
Panel B: Loadings of distance variables on PC_1			
Variable	Loading on *PC1*[b]		
dist_trackit	0.459		
dist_nodeit	0.428		
dist_structit	0.414		
dist_odit	0.465		
dist_markit	0.467		

Notes: *PC* = principal component; IHS = inverse hyperbolic sine.

[a] *PC1* captures 81.8% of the total variance across distance-to-railway measures.

[b] All five distance measures load positively and with similar magnitude on *PC1*, indicating a highly coherent underlying factor representing proximity to the rail network.

Table 3 Summary statistics of AGEB-level variables (2016–2024)

Variable	Description	Unit	Tren Maya municipalities		Rest of the country		p-value difference[a]
			Mean	Std. Dev.	Mean	Std. Dev.	
$luminosity_{it}$	IHS of night-time light intensity per km²	asinh(nW/cm²/sr per km²)	4.38	2.25	3.99	2.31	0.000
$dist_track_{it}$	distance to nearest rail track	km	56.20	64.42	26.75	43.96	0.000
$dist_od_{it}$	distance to nearest OD rail point	km	125.70	116.41	54.34	57.54	0.000
$rail_{it}$	rail accessibility index	PCA-based index	0.71	2.53	-0.03	2.00	0.000
$manuf_{it}$	number of manufacturing establishments	count	5.21	13.95	6.81	19.29	0.000
$const_{it}$	number of construction establishments	count	0.56	1.56	0.32	1.21	0.000
$trans_{it}$	number of transport & warehousing establishments	count	0.43	1.65	0.48	2.24	0.000
$road_{it}$	total road length	km	13.55	26.99	12.92	28.46	0.004

Notes: The unit of observation is AGEB-year. Distances are geodesic (great-circle) distances computed from AGEB centroids. PCA = principal components analysis; IHS = inverse hyperbolic sine.

[a] P-values from tests of equality of means between Tren Maya municipalities and Rest of the country.

Table 4 TWFE estimates: Effect of rail accessibility on night-time luminosity

Rail accessibility measure:	IHS of $dist_track_{it}$		IHS of $dist_od_{it}$		$rail_{it}$	
	(1)	(2)	(3)	(4)	(5)	(6)
β	-0.011	-0.012	-0.021 **	-0.019 *	-0.027 *	-0.023 *
[std. error]	[0.009]	[0.010]	[0.008]	[0.008]	[0.012]	[0.012]
AGEB fixed effects	Yes	Yes	Yes	Yes	Yes	Yes
Year fixed effects	Yes	Yes	Yes	Yes	Yes	Yes
State time trends	Yes	Yes	Yes	Yes	Yes	Yes
Controls	No	Yes	No	Yes	No	Yes
Observations	565,659	447,920	565,659	447,920	565,659	447,920
Number of AGEBs	62,851	56,190	62,851	56,190	62,851	56,190
R-squared (within)	0.282	0.306	0.283	0.307	0.283	0.306
Clusters (municipalities)	2,478	2,478	2,478	2,478	2,478	2,478
corr(u_i, Xb)	0.101	0.245	0.141	0.259	0.263	0.355
rho (share of var. due to FE)	0.995	0.996	0.995	0.996	0.995	0.996

Notes: Robust standard errors clustered at the municipality level are shown in brackets. Significance levels: 0 '***' 0.001 '**' 0.01 '*' 0.05.

Table 5 Dynamic effects of the Tren Maya on luminosity: Event-study estimates (t_0 = 2018)

Treatment group:	AGEBs in Tren Maya municipalities			AGEBs with centroids within a 15-km buffer around the Tren Maya alignment		
	(1)	(2)	(3)	(4)	(5)	(6)
Mean pre-treatment ATT	-0.008 *	-0.031 ***	-0.007	-0.004	-0.001	0.006
	[0.003]	[0.003]	[0.004]	[0.004]	[0.005]	[0.007]
Mean post-treatment ATT	0.023 ***	-0.011 *	0.010	0.041 ***	0.033 ***	0.046 ***
	[0.006]	[0.005]	[0.007]	[0.007]	[0.008]	[0.011]
t = 2018	0.024 ***	0.008 **	0.029 ***	0.021 ***	0.022 ***	0.007
	[0.003]	[0.003]	[0.004]	[0.004]	[0.004]	[0.006]
t = 2019	0.045 ***	0.018 ***	0.035 ***	0.052 ***	0.042 ***	0.035 ***
	[0.005]	[0.004]	[0.006]	[0.005]	[0.006]	[0.009]
t = 2020	-0.039 ***	-0.074 ***	-0.001	-0.037 ***	0.000	-0.001
	[0.006]	[0.005]	[0.007]	[0.007]	[0.008]	[0.012]
t = 2021	0.006	-0.030 ***	-0.044 ***	0.014	-0.028 **	0.001
	[0.007]	[0.006]	[0.008]	[0.008]	[0.009]	[0.013]
t = 2022	0.038 ***	0.001	0.035 ***	0.063 ***	0.066 ***	0.056 ***
	[0.008]	[0.007]	[0.009]	[0.009]	[0.010]	[0.014]
t = 2023	0.064 ***	0.022 **	0.017	0.102 ***	0.069 ***	0.106 ***
	[0.008]	[0.008]	[0.010]	[0.010]	[0.011]	[0.015]
t = 2024	0.022 *	-0.020 *	-0.003	0.069 ***	0.063 ***	0.118 ***
	[0.009]	[0.008]	[0.010]	[0.010]	[0.011]	[0.016]
Observations	565,659	399,341	53,901	565,659	53,901	23,013
Control Group[a]	RoC	RoC	RoSE	RoC	RoSE	RoB
Covariates[b]	No	Yes	No	No	No	No
Pre-trends χ^2	5.955	102.772	2.653	1.163	0.014	0.900
p-value	0.015	0.000	0.103	0.281	0.907	0.343

Notes: Robust standard errors clustered at the municipality level are shown in brackets. Significance levels: 0 '***' 0.001 '**' 0.01 '*' 0.05. Dynamic average treatment effects on the treated (ATT) estimated using the Callaway and Sant'Anna (2021) difference-in-differences estimator with multiple time periods.

[a] The alternative control groups consist of never treated AGEBs in the rest of the country (RoC); never treated AGEBs within other municipalities in southeastern Mexican states (Campeche, Yucatan, Quintana Roo, Tabasco, and Chiapas) not crossed by the Tren Maya rail alignment (RoSE); and the rest of AGEBs within the municipalities crossed by the 15-km buffer (RoB).

[-b] Includes controls for local economic structure (IHS-transformations of $manuf_{it}$, $const_{it}$, and $trans_{it}$) and road infrastructure (IHS-transformation of $road_{it}$).

Table 6 Benchmark elasticities between GDP and night-time luminosity

Study	Unit / Geography	Elasticity[a]
Henderson, et al. (2012)	Long differences (1992/93–2005/06)	0.32
	Country-year panel (global)	0.28
This study[b]	State-year panel for Mexico (2016-2024)	0.18-0.20
Mitnik, et al. (2018)	National time series (Haiti, 29 years)	0.06–0.08

Notes:

[a] Semi-elasticity or elasticity of GDP with respect to night-time luminosity, depending on the functional form.

[b] Elasticity of real gross domestic product at constant 2018 prices with respect to luminosity, measured as the inverse hyperbolic sine of VIIRS light density aggregated at the state level. Estimates obtained from fixed-effects panel regressions with state effects, year effects, and controls (IHS-transformed measures of local economic structure and road infrastructure).

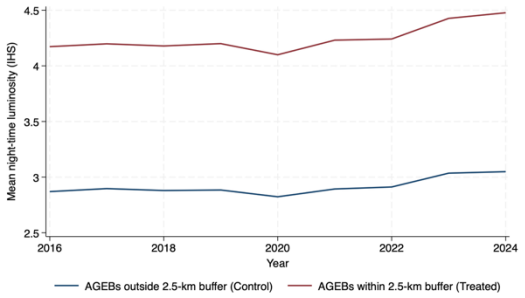
Table 7 Dynamic effects of the Tren Maya on luminosity: State-level spatial heterogeneity (t_0 = 2018)

Treatment group:	AGEBs with centroids within a 2.5-km buffer around the Tren Maya alignment				
Control group:	Never treated AGEBs in the same state				
State:	Campeche	Chiapas	Quintana Roo	Tabasco	Yucatán
Mean pre-treatment ATT	-0.002	0.008	0.002	-0.027	0.029 *
	[0.011]	[0.023]	[0.015]	[0.024]	[0.015]
Mean post-treatment ATT	0.039 *	0.228 ***	0.041	-0.303 ***	0.017
	[0.019]	[0.048]	[0.029]	[0.039]	[0.026]
t = 2018	-0.002	0.082	0.009	-0.240 ***	-0.0002
	[0.011]	[0.048]	[0.018]	[0.024]	[0.013]
t = 2019	0.014	0.084	0.015	-0.249 ***	0.007
	[0.016]	[0.054]	[0.029]	[0.032]	[0.021]
t = 2020	-0.025	0.024	-0.012	-0.291 ***	-0.011
	[0.024]	[0.052]	[0.037]	[0.040]	[0.025]
t = 2021	0.036	0.082	-0.032	-0.350 ***	0.003
	[0.024]	[0.061]	[0.036]	[0.061]	[0.035]
t = 2022	0.029	0.320 ***	-0.023	-0.315 ***	0.029
	[0.024]	[0.063]	[0.040]	[0.055]	[0.036]
t = 2023	0.090 ***	0.464 ***	0.121 **	-0.277 ***	0.048
	[0.026]	[0.044]	[0.044]	[0.046]	[0.036]
t = 2024	0.127 ***	0.541 ***	0.212 ***	-0.403 ***	0.042
	[0.027]	[0.080]	[0.041]	[0.048]	[0.041]
Observations	5,373	18,846	4,747	6,723	10,226
Covariates[a]	No	No	Yes	No	Yes
Pre-trends χ^2	0.019	0.129	0.010	1.256	3.922
p-value	0.892	0.719	0.922	0.263	0.048

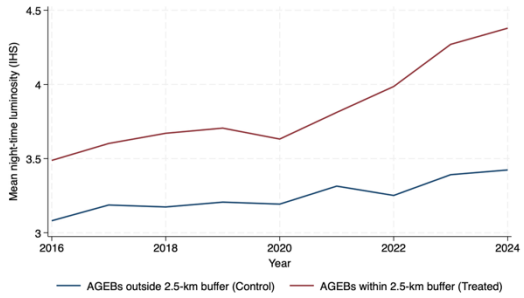
Notes: Robust standard errors clustered at the municipality level are shown in brackets. Significance levels: 0 '***' 0.001 '**' 0.01 '*' 0.05. Dynamic average treatment effects on the treated (ATT) estimated using the Callaway and Sant'Anna (2021) difference-in-differences estimator with multiple time periods.

[a] Includes controls for local economic structure (IHS-transformations of $manuf_{it}$, $const_{it}$, and $trans_{it}$) and road infrastructure (IHS-transformation of $road_{it}$).

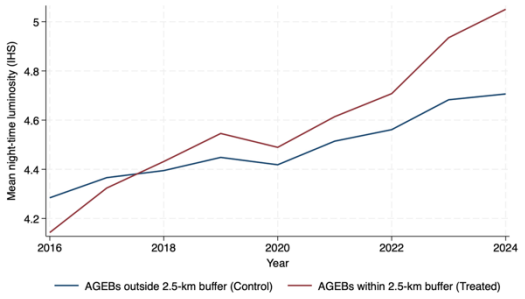
APPENDIX



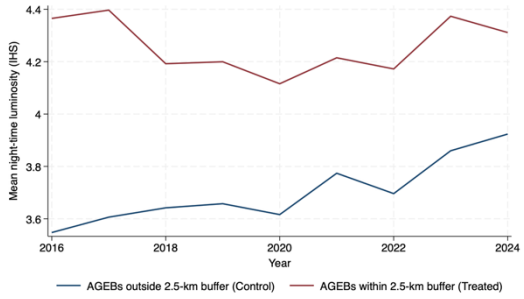
Campeche



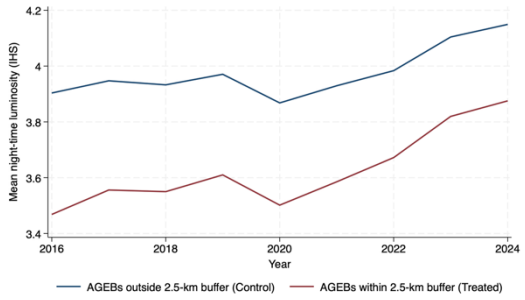
Chiapas



Quintana Roo



Tabasco



Yucatán

Figure A1 Evolution of mean night-time luminosity in the Mexican southeastern states

Notes: Mean night-time luminosity (inverse hyperbolic sine transformation) for AGEBs located within and outside a 2.5-km geodesic buffer around the Tren Maya alignment, separately for each southeastern state. Treated AGEBs correspond to those whose centroids fall within the buffer, while control (never treated) AGEBs are those located outside the buffer within the same state. Luminosity is averaged across AGEBs for each group and year.

Table A1 Dynamic effects of the Tren Maya on luminosity: Event-Study estimates with alternative buffer scenarios (t_0 = 2018)

Treatment group:	AGEBs with centroids within a 5-km buffer around the Tren Maya alignment			AGEBs with centroids within a 10-km buffer around the Tren Maya alignment			AGEBs with centroids within a 20-km buffer around the Tren Maya alignment		
	(1)	(2)	(3)	(4)	(5)	(6)	(7)	(8)	(9)
Mean pre-treatment ATT	-0.019 ***	-0.005	0.019 **	-0.018 ***	-0.001	0.024 ***	-0.007	-0.005	0.005
	[0.005]	[0.006]	[0.006]	[0.004]	[0.005]	[0.006]	[0.004]	[0.004]	[0.006]
Mean post-treatment ATT	0.026 **	0.022 *	0.044 ***	0.014	0.012	0.047 ***	0.031 ***	0.022 ***	0.026 **
	[0.010]	[0.010]	[0.012]	[0.007]	[0.008]	[0.010]	[0.006]	[0.007]	[0.010]
t = 2018	-0.007	-0.010	-0.023 ***	0.005	0.004	-0.008	0.023 ***	0.026 ***	0.024 ***
	[0.005]	[0.006]	[0.007]	[0.004]	[0.004]	[0.006]	[0.003]	[0.004]	[0.006]
t = 2019	0.016 *	-0.004	-0.007	0.023 ***	0.008	0.006	0.048 ***	0.040 ***	0.035 ***
	[0.008]	[0.008]	[0.010]	[0.006]	[0.006]	[0.009]	[0.005]	[0.006]	[0.008]
t = 2020	-0.078 ***	-0.033 **	-0.004	-0.073 ***	-0.027 ***	0.010	-0.041 ***	-0.005	-0.002
	[0.011]	[0.011]	[0.012]	[0.007]	[0.008]	[0.010]	[0.007]	[0.008]	[0.010]
t = 2021	-0.009	-0.038 **	0.017	-0.018 *	-0.048 ***	0.015	0.008	-0.040 ***	-0.012
	[0.012]	[0.013]	[0.014]	[0.009]	[0.010]	[0.012]	[0.007]	[0.008]	[0.012]
t = 2022	0.046 ***	0.048 ***	0.048 **	0.033 ***	0.040 ***	0.053 ***	0.048 ***	0.049 ***	0.022
	[0.013]	[0.014]	[0.016]	[0.010]	[0.011]	[0.014]	[0.008]	[0.009]	[0.013]
t = 2023	0.119 ***	0.093 ***	0.124 ***	0.078 ***	0.054 ***	0.113 ***	0.082 ***	0.044 ***	0.050 ***
	[0.014]	[0.015]	[0.017]	[0.011]	[0.012]	[0.015]	[0.009]	[0.010]	[0.014]
t = 2024	0.097 ***	0.102 ***	0.156 ***	0.048 ***	0.055 ***	0.142 ***	0.049 ***	0.038 ***	0.064 ***
	[0.015]	[0.016]	[0.018]	[0.011]	[0.012]	[0.015]	[0.009]	[0.011]	[0.014]
Observations	399,341	39,413	13,217	399,341	39,413	13,774	565,659	53,901	24,912
Control Group[a]	RoC	RoSE	RoB	RoC	RoSE	RoB	RoC	RoSE	RoB
Covariates[b]	Yes	Yes	Yes	Yes	Yes	Yes	No	No	No
Pre-trends χ^2	13.274	0.788	9.345	23.140	0.063	14.566	3.841	1.270	0.717
p-value	0.000	0.375	0.002	0.000	0.802	0.000	0.050	0.260	0.397

Notes: Robust standard errors clustered at the municipality level are shown in brackets. Significance levels: 0 '***' 0.001 '**' 0.01 '*' 0.05. Dynamic average treatment effects on the treated (ATT) estimated using the Callaway and Sant'Anna (2021) difference-in-differences estimator with multiple time periods.

[a] The alternative control groups consist of never treated AGEBs in the rest of the country (RoC); never treated AGEBs within other municipalities in southeastern Mexican states (Campeche, Yucatan, Quintana Roo, Tabasco, and Chiapas) not crossed by the Tren Maya rail alignment (RoSE); and the rest of AGEBs within the municipalities crossed by the buffer (RoB).

[b] Includes controls for local economic structure (IHS-transformations of $manuf_{it}$, $const_{it}$, and $trans_{it}$) and road infrastructure (IHS-transformation of $road_{it}$).

Table A2 Dynamic effects of the Tren Maya on luminosity: Event-Study estimates ($t_0 = 2020$)

Treatment group:	AGEBs in Tren Maya municipalities				AGEBs with centroids within a 15-km buffer around the Tren Maya alignment		
	(1)	(2)	(3)	(4)	(4)	(5)	(6)
Mean pre-treatment ATT	0.012 ***	-0.003	0.009 ***	-0.005 *	0.0001	-0.0002	-0.007
	[0.002]	[0.002]	[0.003]	[0.002]	[0.002]	[0.002]	[0.004]
Mean post-treatment ATT	-0.026 ***	-0.038 ***	-0.034 ***	-0.052 ***	-0.026 ***	-0.026 ***	-0.011
	[0.005]	[0.004]	[0.006]	[0.006]	[0.005]	[0.006]	[0.012]
t = 2020	-0.083 ***	-0.092 ***	-0.037 ***	-0.049 ***	-0.096 ***	-0.044 ***	-0.025 **
	[0.003]	[0.003]	[0.004]	[0.004]	[0.003]	[0.004]	[0.009]
t = 2021	-0.039 ***	-0.049 ***	-0.079 ***	-0.093 ***	-0.049 ***	-0.081 ***	-0.061 ***
	[0.004]	[0.004]	[0.006]	[0.006]	[0.005]	[0.006]	[0.015]
t = 2022	-0.006	-0.019 ***	0.000	-0.018 **	-0.005	0.006	-0.018
	[0.005]	[0.005]	[0.007]	[0.007]	[0.005]	[0.007]	[0.014]
t = 2023	0.019 **	0.005	-0.018 *	-0.038 ***	0.028 ***	0.000	0.025
	[0.006]	[0.006]	[0.008]	[0.008]	[0.007]	[0.008]	[0.014]
t = 2024	-0.023 ***	-0.036 ***	-0.038 ***	-0.061 ***	-0.007	-0.010	0.026
	[0.007]	[0.007]	[0.008]	[0.009]	[0.008]	[0.009]	[0.016]
Observations	565,659	436,300	53,901	42,896	436,300	42,896	17,295
Control Group[a]	RoC	RoC	RoSE	RoSE	RoC	RoSE	RoB
Covariates[b]	No	Yes	No	Yes	Yes	Yes	Yes
Pre-trends χ^2	111.951	136.909	66.415	27.709	105.082	6.040	3.903
p-value	0.000	0.000	0.000	0.000	0.000	0.110	0.272

Notes: Robust standard errors clustered at the municipality level are shown in brackets. Significance levels: 0 '***' 0.001 '**' 0.01 '*' 0.05. Dynamic average treatment effects on the treated (ATT) estimated using the Callaway and Sant'Anna (2021) difference-in-differences estimator with multiple time periods.

[a] The alternative control groups consist of never treated AGEBs in the rest of the country (RoC); never treated AGEBs within other municipalities in southeastern Mexican states (Campeche, Yucatan, Quintana Roo, Tabasco, and Chiapas) not crossed by the Tren Maya rail alignment (RoSE); and the rest of AGEBs within the municipalities crossed by the 15-km buffer (RoB).

[b] Includes controls for local economic structure (IHS-transformations of $manuf_{it}$, $const_{it}$, and $trans_{it}$) and road infrastructure (IHS-transformation of $road_{it}$).